Monthly Notices
of the
ROYAL ASTRONOMICAL SOCIETY

MNRAS **464,** 2557–2564 (2017)
Advance Access publication 2016 October 8

doi:10.1093/mnras/stw2585

The fate of exomoons in white dwarf planetary systems

Matthew J. Payne,[1]★ Dimitri Veras,[2] Boris T. Gänsicke[2] and Matthew J. Holman[1]

[1]*Harvard–Smithsonian Center for Astrophysics, 60 Garden Street, MS 51, Cambridge, MA 02138, USA*
[2]*Department of Physics, University of Warwick, Coventry CV4 7AL, UK*

Accepted 2016 October 6. Received 2016 October 4; in original form 2016 March 30; Editorial Decision 2016 October 4

ABSTRACT

Roughly 1000 white dwarfs are known to be polluted with planetary material, and the progenitors of this material are typically assumed to be asteroids. The dynamical architectures which perturb asteroids into white dwarfs are still unknown, but may be crucially dependent on moons liberated from parent planets during post-main-sequence gravitational scattering. Here, we trace the fate of these exomoons, and show that they more easily achieve deep radial incursions towards the white dwarf than do scattered planets. Consequently, moons are likely to play a significant role in white dwarf pollution, and in some cases may be the progenitors of the pollution itself.

Key words: methods: numerical – celestial mechanics – planets and satellites: dynamical evolution and stability.

1 INTRODUCTION

What is the long-term fate of planetary systems? Abundant observations reveal substantial clues (Farihi 2016), but theoretical explanations are lacking (e.g. Veras 2016a). We know that planetary systems exist around evolved stars, including both giant stars[1] and white dwarfs (e.g. Vanderburg et al. 2015). White dwarf planetary systems feature some combination of atmospheric metal pollution (obtained with spectroscopic absorption lines); orbiting bodies observed through transit photometry; and debris discs with dust and gas from infrared excesses, spectroscopic emission features and Doppler tomography.

One feature common to all of these white dwarf systems is metal pollution (see Farihi 2016 and Veras 2016a for review articles). White dwarf atmospheres break up accreted material into their constituent chemical elements and then stratify them according to weight (Schatzman 1945). Consequently, the visible uppermost layers of their atmosphere should contain only a combination of hydrogen, helium and possibly carbon. In reality, between one-quarter and one-half of all known white dwarfs (Zuckerman et al. 2003, 2010; Koester, Gänsicke & Farihi 2014) harbour up to 18 elements (Klein et al. 2010, 2011; Gänsicke et al. 2012; Jura et al. 2012; Xu et al. 2013, 2014; Wilson et al. 2015), providing evidence of frequent, ongoing accretion of fragmentary planetary material on to white dwarfs. The details of this chemistry and implications for planet formation are reviewed in Jura & Young (2014). In total, about 1000 white dwarfs are known to be polluted with metals (Dufour et al. 2007; Kleinman et al. 2013; Gentile Fusillo et al. 2015; Kepler et al. 2015, 2016).

About 40 of these polluted white dwarfs are known to be surrounded by dusty compact debris discs with radial extents of about 1 $R_\odot$ (Farihi 2016). These discs lie within the disruption, or Roche radius, of the white dwarf, and hence are composed of broken-up fragments. The distance at which sublimation occurs often lies within this range, producing gas. In eight cases, this gas is observable (Gänsicke et al. 2006, 2008; Gänsicke, Marsh & Southworth 2007; Gänsicke 2011; Dufour et al. 2012; Farihi et al. 2012; Melis et al. 2012; Guo et al. 2015) and can constrain the disc geometry, which may be eccentric and non-axisymmetric (Manser et al. 2016).

A long-term goal has been to combine these detections with the detection of an orbiting planet (Mullally et al. 2008; Hogan, Burleigh & Clarke 2009; Debes et al. 2011; Faedi et al. 2011; Steele et al. 2011; Fulton et al. 2014; Sandhaus et al. 2016). A recent success is WD 1145+017 (Vanderburg et al. 2015), a white dwarf which is both polluted and bears a debris disc, and which has recently been shown to also host disintegrating planetesimals. Hourly changes in the shape and depth of the transit light curves of the white dwarf WD 1145+017 have invigorated the post-main-sequence planetary community, motivating a large-scale observational effort (Alonso et al. 2016; Croll et al. 2016; Gänsicke et al. 2016; Gary et al. 2016; Rappaport et al. 2016; Redfield et al. 2016; Xu et al. 2016) and dedicated attempts to explain these observations (Gurri, Veras & Gänsicke 2017; Veras et al. 2016c). The parallel understanding of the state-of-the-art dynamical and theoretical aspects of post-main-sequence planetary science is summarized in Veras (2016a).

Traditionally, asteroids have been invoked as the progenitors of the disintegrating planetesimals, debris discs and metal pollution (Graham et al. 1990; Jura 2003; Bear & Soker 2013). This notion was quantified by Bonsor, Mustill & Wyatt (2011), Debes, Walsh & Stark (2012) and Frewen & Hansen (2014), who showed how

★E-mail: matthewjohnpayne@gmail.com, mpayne@cfa.harvard.edu

[1] Sabine Reffert maintains a data base at http://www.lsw.uni-heidelberg.de/users/sreffert/giantplanets.html to which we refer the reader for further references to numerous individual discovery papers.

a planet can perturb an asteroid in the vicinity of a white dwarf, as long as some configurations are avoided (Antoniadou & Veras 2016). After tidally breaking up (Debes et al. 2012; Veras et al. 2014b), the resulting debris is then circularized by stellar radiation (and possibly additional mechanisms, such as gas drag; Veras et al. 2015b), forming a disc which eventually accretes on to the white dwarf (Rafikov 2011a,b; Rafikov & Garmilla 2012; Metzger, Rafikov & Bochkarev 2012).

However, moons liberated during planet–planet scattering in white dwarf systems, a common phenomenon (Payne et al. 2016), may change this general picture in two ways: (1) the moons themselves might accrete directly on to the white dwarf, or (2) the moons can become minor planets and change the efficiency with which asteroids can be perturbed on to the white dwarf. Regarding the first point, the internal composition of the moons may be similar to those of the asteroid families inferred from the polluted debris. For the second point, a chain of large (moon-sized or planet-sized) bodies may help perturb an asteroid (Bonsor & Wyatt 2012) into a target as small as a white dwarf, particularly since the inner few au in white dwarf systems will have been cleared out by the increase in size of the star along the giant branch (Villaver & Livio 2009; Kunitomo et al. 2011; Mustill & Villaver 2012; Adams & Bloch 2013; Nordhaus & Spiegel 2013; Villaver et al. 2014; Staff et al. 2016).

Here, we track the trajectories of moons which escape from the clutches of their parent planet after the star has become a white dwarf, in order to better understand their role in the pollution process. In Section 2, we describe the planet-based simulations which we use as a foundation for our study. Then, in Section 3, we describe how we add moons into the simulations. Section 4 presents our results, and we conclude in Section 5.

2 LONG-TERM, PLANET-ONLY SIMULATIONS OF PLANET–PLANET SCATTERING

Simulating the evolution of multiple planets across all phases of stellar evolution is challenging due to computational limitations and the necessity of combining stellar and planetary evolution. The addition of moons makes this prospect effectively impossible with current technology because they prohibitively decrease the timestep.

Consequently, we must rely on multiplanet simulations *without* moons prior to the white dwarf phase, and then add moons in only at later stages, once it is known that planetary instability is guaranteed on a short time-scale. Only a few studies have integrated suites of self-consistent multiplanet simulations across the main sequence, giant branch and white dwarf phases. Veras et al. (2013) and Mustill, Veras & Villaver (2014) performed two-planet and three-planet simulations, respectively. However, for computational reasons, both studies modelled stars with main-sequence masses of $3\,M_{\odot}$ or greater. Alternatively, Veras (2016b) modelled the fate of Solar system analogues (with a $1.0\text{-}M_{\odot}$ star); however, he had to skip most of the main sequence. The present-day population of white dwarfs corresponds to a progenitor mass range of 1.5–$2.5\,M_{\odot}$, with a peak at around $2.0\,M_{\odot}$ (e.g. fig. 1 of Koester et al. 2014). With this mass range in mind, both Veras & Gänsicke (2015) and Veras et al. (2016a) simulated systems with four or more planets across all phases of stellar evolution, including the entire main sequence and giant branch phases.

We rely on simulations from both of these studies, in which Veras & Gänsicke (2015) adopted equal-mass planets, and Veras et al. (2016a) investigated unequal-mass planets within the same system. In these simulations, packed systems of planets were integrated for $>10^{10}$ yr, with the central star initially being on the main sequence, then passing through the giant branch (and hence losing mass), before settling into the white dwarf phase. The stellar mass-loss causes the planetary semimajor axes to expand, and can trigger late instability. We use here an ensemble of 119 of these simulations, which all featured planets that remained stable and packed throughout the main sequence and giant branch phase, before suffering their first mutual close encounter along the white dwarf phase. These 119 simulations include four- and ten-planet systems, as well as planets with the mass of Jupiter, Saturn, Neptune, Uranus, Earth, and planets with masses down to 0.046 Earth masses. Payne et al. (2016) investigated a subset of these simulations and determined that the distribution of close approaches between the *planets* of these simulations could efficiently eject moons from a wide range of circumplanetary orbits. In this investigation, we wish to understand where these moons ultimately go to, once they are liberated from circumplanetary orbit.

3 ADDING MOONS TO LONG-TERM SIMULATIONS OF PLANET–PLANET SCATTERING

Here, we discuss strategically inserting moons into the systems from Veras & Gänsicke (2015) and Veras et al. (2016a) at times and locations which would provide us with the greatest insight.

3.1 Timescales and timesteps

The planet-only simulations described in Section 2 can be completed relatively rapidly; the timestep required to resolve a system scales with the time-scale of the shortest orbit: for planet-only simulations with typical orbits at many au, orbits typically have periods of a few years, and typical timesteps required to resolve orbits can be many days.

Adding moons around any planet in such a simulation can cause significant additional computational strain: the orbital period of moons can easily be a few days (or less), requiring timesteps which are measured in hours in order to resolve the system. This setup ultimately causes typical planet-only simulation run-times to increase by about two orders of magnitude.

A concrete example is the following: numerically integrating a four-planet simulation of the kind illustrated in Fig. 1 for a short time (10^4 yr) takes far less than 1 s with only planets in the simulation, but $\sim$200 s when one moon is added on to each planet (see Section 3.2 for typical moon parameters). These time-scales make it impractical to simulate systems for billions of years, during which moons remain bound to their parent planet.

Two practical considerations allow us to side-step this problem. (i) We know the approximate time at which planets start to interact strongly, i.e. the time of the first ‘close encounter’. Consequently, we can ignore the system’s previous history: the timespan over which planets remain bound and ordered. Our simulation selection guarantees that this span includes the entire main sequence and giant branch lifetimes, and at least some amount of time on the white dwarf phase. We know that the moons will remain bound to their parent planets during these earlier phases with few exceptions (Payne et al. 2013).

(ii) While the moons are bound, timesteps must remain short, but if the moons become unbound from their parent planet and move on to planet-like orbits, then the simulation timestep can increase by orders of magnitude, allowing simulations to rapidly progress.

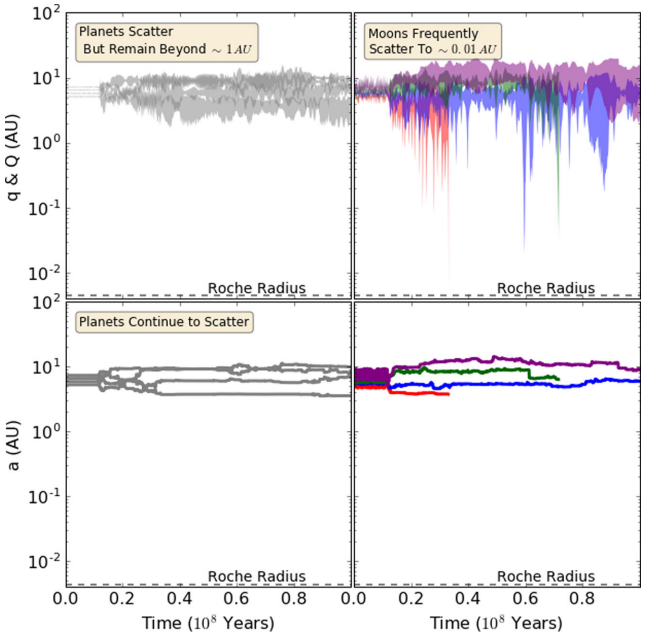

Figure 1. Example of moon and planet evolution after moons have been liberated. We plot the semimajor axes (bottom) and pericentres and apocentres (top) of four Earth-mass planets (grey, left) and four (test particle) moons (colours, right). The semimajor axes are plotted using solid lines, while the pericentres and apocentres are plotted using filled ranges. The moons are initially bound to the planets, one moon per planet. After $\sim 10^7$ yr, planet–planet scattering commences, unbinding all four moons (in this example) from their parent planets and liberating them into white dwarf-centric orbits. The planets remain relatively distant from the white dwarf (beyond $\sim$1 au), but the moons are highly scattered, frequently coming within $\sim$0.1 au of the WD. The red moon comes within a factor of a few of the disruption, or Roche, distance (plotted as a grey dashed line, assuming a density of 3 g cm^{-3}) at closest approach.

3.2 Insertion point

In order to identify the first close encounter time, we use a simple, approximate definition of orbit crossing: when, for an adjacent pair of planets, the pericentre of the outer orbit overlaps with the apocentre of the inner orbit. This method ignores subtleties associated with resonant orbits, but suffices for our purpose.

After identifying the first close encounter time, we extract the state of the system (masses, positions and velocities of all bodies) at a time 10^6 yr prior to the onset of orbit crossing. We adopt this previous timestep as our new 'time-zero', and add moons to the simulation at this time in the manner detailed in Section 3.3.

We then integrate the simulations forward through the first close planet–planet encounter, and onwards through the next 10^8 yr of strong planet–planet interactions as the planets, now on crossing orbits, repeatedly scatter in the manner illustrated in, for example, fig. 1 of Veras & Gänsicke (2015) and Fig. 1 of this paper. Further details and discussion are provided in Sections 3.4 and 6.

We note that the first close planet–planet scattering encounter (and hence possible moon liberation) should be expected to occur sometime *after* the onset of orbit crossing.

3.3 Moon properties

We add one moon to each of the planets in the simulation. The moon is integrated as a test particle with mass $m_\mathrm{m} = 0$. The initial semimajor axis of the moon with respect to the planet, a_m, in units of the parent planet's instantaneous Hill radius, r_H, is chosen randomly such that the distribution of the semimajor axes is uniform in log-space in the range $0.04 < a_\mathrm{m}/r_\mathrm{H} < 0.4$. Although we know from Payne et al. (2016) that moons can be liberated even from orbits with $a_\mathrm{m}/r_\mathrm{H} < 10^{-2}$, here we are particularly interested in the *fate* of moons once liberated, rather than the fine details of which moons in particular will be liberated. As such, we choose to focus our attention on moons which occupy orbits with semimajor axes in the range $0.04 < a_\mathrm{m}/r_\mathrm{H} < 0.4$. Such a range of semimajor axes was chosen to ensure that (1) the outer edge of the distribution is just interior to the stability boundary at $\sim 0.5 r_\mathrm{H}$, and (2) the inner edge of the distribution is sufficiently distant from the planet to make the orbital period manageably long.

The inclinations i_m (of a moon with respect to its parent planet) were drawn randomly from a uniform distribution and have all values within 1° of the plane of the planetary orbits (which themselves *initially* had mutual inclinations within about a degree at the start of the simulations, but by the time we insert the moons, have started to excite larger inclinations). The small but non-zero inclination guarantees that the systems are fully three dimensional in their interactions, while the low inclinations prevent any unwanted loss of moons via the Kozai mechanism. Once liberated from their parent planets, the inclination of the moons becomes highly non-coplanar, erasing the memory of their initial plane (see Fig. 4).

The longitude of ascending node, argument of pericentre and mean anomaly of each moon were all drawn from a uniform distribution between 0° and 360°.

3.4 New integrations

The integrations were performed using the Bulirsch–Stoer algorithm from the MERCURY *N*-body package of Chambers (1999) with an accuracy of 10^{-13} and a runtime of 10^8 yr. Such a runtime is sufficient to guarantee multiple close planet–planet encounters, while remaining computationally tractable for the short timesteps required for bound moons. We refer the reader to Fig. 1 for an example of the multiple close encounters which can occur during the 10^8-yr simulation, clearly visible as the semimajor axes of the planets repeatedly perform discontinuous jumps in semimajor axis.

Because the integrations took place on the white dwarf phase, it was not necessary to take stellar evolution into consideration. Note that unlike main sequence and giant branch stars, white dwarfs do not have winds. Hence, orbiting bodies are not affected by stellar mass-loss (see section 4 of Veras 2016a). Objects under 1000 km in size would be affected by radiation from the parent star on the giant branch phase (Veras, Eggl & Gänsicke 2015a), but not around a white dwarf unless the object was a boulder (approximately 0.1 m) or smaller (Veras et al. 2015b) or was outgassing significant volatiles (Veras, Eggl & Gänsicke 2015c). Here, we consider just point-mass gravitational dynamics.

Note that in Payne et al. (2016), we illustrated the range of moon semimajor axes (with respect to their parent planets) from which planet–planet scattering can efficiently cause moons to be liberated from their parent planet into heliocentric orbits. A future study will provide additional details of the exact dependences of this liberation on the properties of the scattering planets as well as the initial orbits of the moons. However, the point of the integrations in this study is to demonstrate what happens to the moons once they are liberated from their parent planets. We emphasize that once the moons are liberated into heliocentric orbits, their heliocentric orbits, by definition, must be planet crossing, hence their subsequent evolution will be chaotic, driven by multiple hard-scattering events (during close approaches

with the massive planets in the system) which naturally wipe all memory of the moons' initial circumplanetary orbits. We wish to use these simulations to understand the range of distances through which this hard scattering drives the moons, and to understand whether this is different to that of the planets from which they are liberated.

4 NUMERICAL INTEGRATION RESULTS

First, consider the evolution of a single system, as in Fig. 1. In that system, four Earth-mass planets orbiting a 1.5-$M_\odot$ main-sequence star remain stable until the white dwarf phase. About 1 Myr before the planets first cross orbits, we added one moon to each planet and then integrated the system forward for 10^8 yr. What is plotted is the subsequent evolution. The moons were initially placed at distances of $a/r_{\rm H} = 0.13$, 0.24, 0.06 and 0.05 from the planets (one moon per planet) in planet order from the star.

After about 10 Myr, the close encounters (between planets) result in strong scattering events which (in this example) liberate all four moons within a short period of time. These moons become new minor planets themselves, orbiting the white dwarf instead of any of the extant planets. Now, the system effectively has eight planets. Three of the former moons (blue, red and green) change their orbits in such a way so as to achieve pericentres below 0.1 au, an order of magnitude less than the pericentres of the Earth-mass planets.

Now consider the results from our ensemble of 119 systems. Not all moons are liberated from their parent planets and stay in the system. Fig. 2 reveals the different possible qualitative outcomes, as a function of separation from parent planet. Because many moons remain bound, over a wide range of $r/r_{\rm H}$, at 10^8 yr, they will be susceptible to liberation if further planet–planet scattering encounters occur (Payne et al. 2016). As planet–planet scattering around WDs can occur over Gyr time-scales (far longer than examined here, see fig. 1 of Veras & Gänsicke 2015), many more close encounters will occur, making it extremely likely that yet more moons will be liberated from their parent planets at future times. We note that the fine details of an individual planet–planet scattering encounter (e.g. the distance of close approach) are essentially stochastic, so over time, a greater range of planet–planet encounter parameters will be explored, leading to an increased probability of more tightly bound moons being ejected as time goes on. However, once the moons are ejected from their parent planet, all memory of their initial conditions is erased by strong scattering between the liberated moons (now minor planets) and the large planets whose orbits they cross.

The moons of greatest interest are those which have escaped from their parent planet, but not from the white dwarf system. The minimum orbital pericentres of these moons are perhaps the most consequential parameters for white dwarf pollution. Hence, in Fig. 3, we illustrate the distribution of pericentres, showing that ∼15 per cent of moons come within 0.1 au, and ∼5 per cent come within 10^{-2} au. Also plotted are the minimum orbital pericentres of the parent planets: comparing both pericentres illustrates that moons are much more effective at achieving intrusive radial incursions towards the white dwarf than moons; this is the key result of this work. At the bottom of Fig. 3, we plot the cumulative histogram of the time spent with a given pericentre over all simulations. The planets (thin dashed line) spend no significant amount of time inside *an*au, while the moons effectively display a power-law dependence, spending $\sim 10^5$ yr inside 0.1 au, and $\sim 10^4$ yr inside 0.01 au out of this 10^8-yr simulation.

Even slight initial inclinations of less than a degree can, after scattering, generate inclinations spanning the entire range (e.g. Veras &

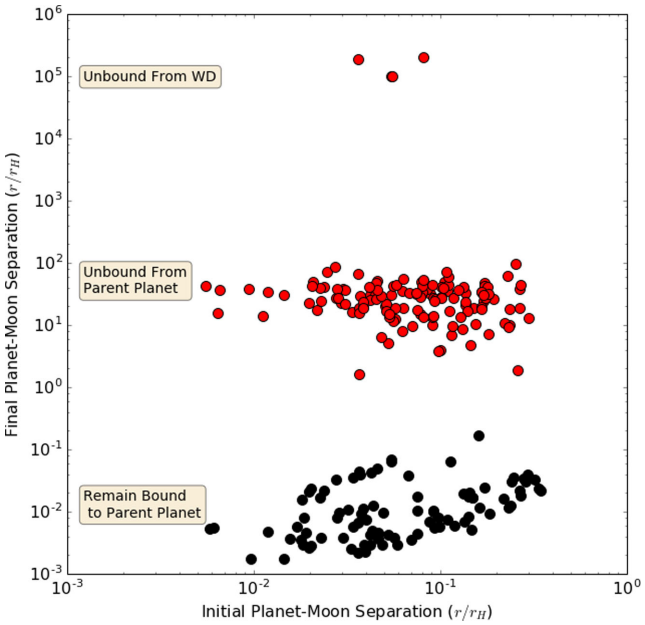

Figure 2. Distribution of separations between moons and their parent planets. On the horizontal axis, we plot the initial separation, and on the vertical axis we plot the final separation after 10^8 yr of simulation. We see that the moons split into two main groups, with the moons at the bottom (black dots) being those that remain bound to their parent planet, while those at the top (in red) have become unbound from their parent planet and have moved into heliocentric (or white dwarf-centric) orbits (of which three have been completely ejected from the white dwarf system). It is highly plausible that with increased simulation time, additional moons will become unbound, as (a) many moons remain bound at a wide range of $r/r_{\rm H}$ values, and (b) planet–planet encounters continue over Gyr time-scales (see Fig. 1, and fig. 1 of Veras & Gänsicke 2015).

Armitage 2005; Raymond, Armitage & Gorelick 2010; Matsumura, Ida & Nagasawa 2013; Li et al. 2014). Consequently, in Fig. 4, we compare the inclinations of the scattered planets and scattered moons. The figure demonstrates that moons easily achieve higher inclinations, including near-polar and retrograde inclinations.

As seen in Fig. 1, as the white dwarf continues to cool, the system will continue to dynamically evolve, as the planets and liberated moons occupy crossing orbits. The chaotic evolution driven by hard scattering between planets and liberated moons causes the power-law distribution of pericentres in the bottom of Fig. 2. This means that over longer time periods, it becomes increasingly likely that some moons will eventually come close to, and possibly collide with, the white dwarf.

5 MOONS AND POLLUTION

In Section 4, we demonstrated that liberated moons which scatter around the system in the manner depicted in Fig. 1 can spend a non-trivial amount of time within 0.1 au or even as close as 0.01 au.

5.1 Tidal disruption

At close pericentre approaches, moons may be subjected to both tidal interactions with the star, and radiative effects, neither of which were modelled in Section 4.

The effect of tides is strongly dependent on the internal composition of the exomoons. Differing rheologies can cause the circularization time-scale to vary by orders of magnitude (Henning

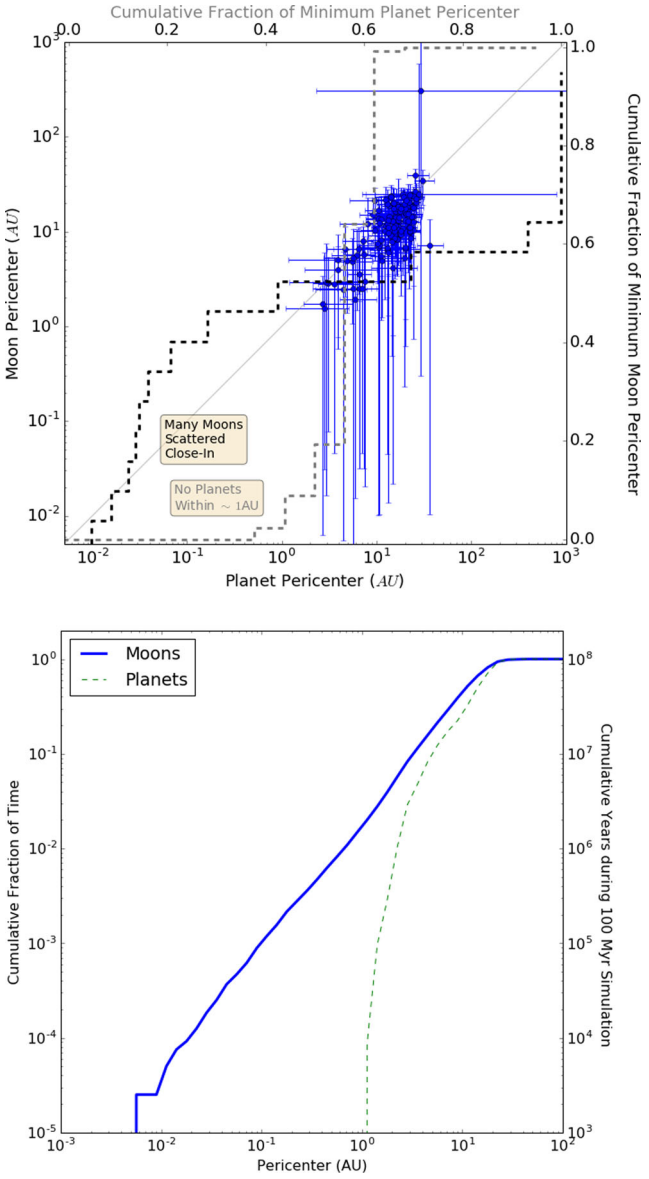

Figure 3. Top: Distribution of pericentres for the moons from Fig. 2, which are unbound from their parent planets but still bound to the white dwarf system. On the horizontal axis, we plot the pericentres of the parent planets, while on the vertical axis we plot the pericentres of the moons. The points indicate the median pericentre values for each, while the error bars indicate the minimum and maximum pericentres ever achieved by the object. We see that for these simulations the planets never come inside ∼1 au, while the moons frequently come in to ∼0.01 au (a few Roche radii). The dashed lines provide cumulative histograms of the minimum pericentre distributions for the planets (grey) and moons (black), with the scales being on the right and top axes, respectively. Bottom: Cumulative fraction of time with a given pericentre. The moon (thick blue line) spends a much greater fraction of time at small pericentres than do the planets (thin dashed line).

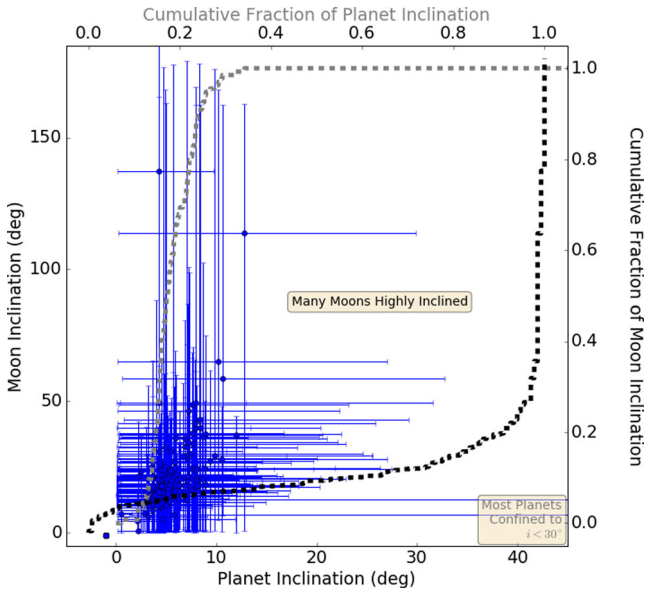

Figure 4. Distribution of inclinations for the moons from Fig. 2 which are unbound from their parent planets but still bound to the white dwarf system. On the horizontal axis, we plot the inclination of the parent planets, while on the vertical axis we plot the inclination of the moons. The points indicate the median inclination values for each, while the error bars indicate the minimum and maximum inclination ever observed for the object in the simulations. We see that for these simulations the planets generally remain confined within $\lesssim 30^\circ$, while the moons frequently become highly inclined or even retrograde. The dashed lines provide cumulative histograms of the inclination distributions for the planets (grey) and moons (black), with the scales being on the right and top axes, respectively.

& Hurford 2014), and therefore must be treated on a case-by-case basis. Simple tidal models such as the constant geometric lag model have proven false (Efroimsky & Makarov 2013) and cannot be used for quantification.

However, it is possible that radiation and tides might act to circularize and shrink the orbit, if not destroy the moon through overspinning (Veras, Jacobson & Gänsicke 2014c). To demonstrate the plausibility of this scenario, we consider the tidal disruption radius, r_c, described in equation (2) of Veras et al. (2014b):

$$\frac{r_c}{\mathrm{R}_\odot} = C \left(\frac{M_{\mathrm{WD}}}{0.6\,\mathrm{M}_\odot}\right)\left(\frac{\rho}{3\,\mathrm{g\,cm^{-3}}}\right)^{-1/3}, \quad (1)$$

where C is a constant ranging from about 0.85 to 1.89 (Bear & Soker 2013), M_{WD} is the mass of the WD and ρ is the assumed density of the moon. For $C = 1.89$ and $\rho = 1.8\,\mathrm{g\,cm^{-3}}$ (the same as Callisto),

$$r_c \approx 2.2\,\mathrm{R}_\odot \approx 0.011\,\mathrm{au}. \quad (2)$$

As we illustrated in Fig. 3, moons do indeed get scattered inside this critical radius for tidal disruption. Hence, for the example coefficients chosen, these moons would be tidally disrupted as they passed within r_c close to pericentre passage.

The disruption of a single moon, which must initially be on a highly eccentric orbit in order to enter the disruption sphere, results in a highly eccentric ring of debris (Veras et al. 2014b). The subsequent evolution of the particles in this eccentric debris ring is strongly dependent on particle size: Veras et al. (2015b) demonstrate that circularization of these orbits occurs efficiently for fragments in the size range 10^{-5}–10^{-1} m, on time-scales many orders of magnitude shorter than the cooling age of the white dwarf, due solely to the radiation effects from the white dwarf acting on the fragments.

5.2 Scattering of small bodies

For those moons which do *not* directly encounter the tidal disruption radius of the white dwarf, they may still be able to contribute to the

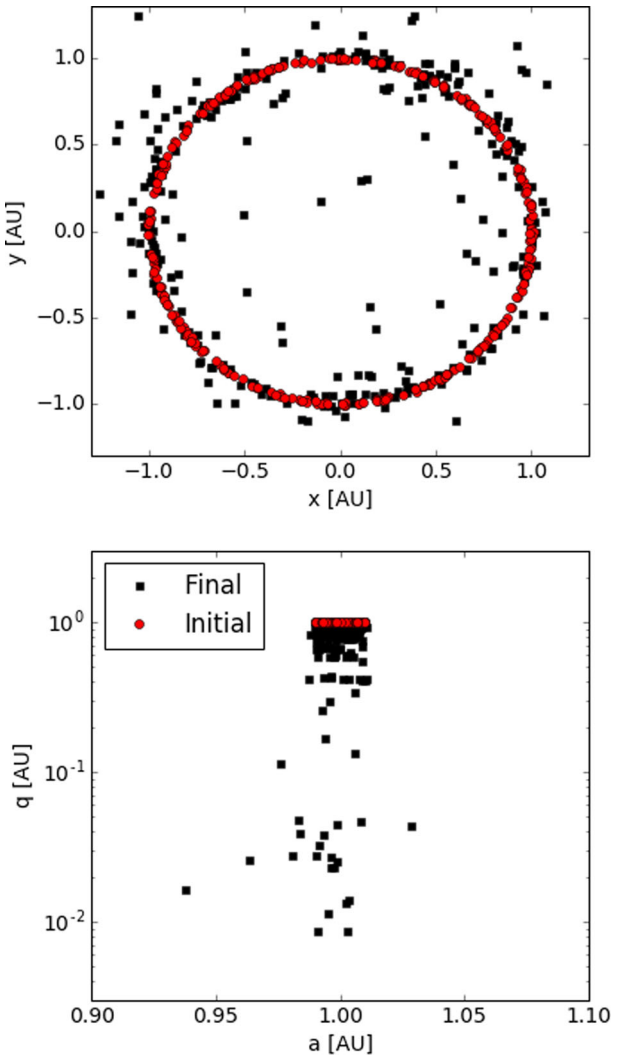

Figure 5. Scattering of interior belt by eccentric moons. We add a belt of test particles to the simulation illustrated in Fig. 1. The belt is initially located at $a_{\rm belt} = 1.0$ au (red circles). The final state of the belt is plotted using black squares. In the top panel, we show a Cartesian snapshot of the planet, illustrating the initial conditions and the final positions at $t = 10^7$ yr. In the bottom panel, we show the a and q values. The belt is excited to pericentres ∼0.01 au within 10 Myr.

pollution *indirectly* by acting as a perturbing mechanism for smaller bodies to be scattered close to the white dwarf.

If we consider a population of small bodies (analogous to the asteroid belt) distributed in an annulus with semimajor axis $a_{\rm belt}$, then they will initially be unperturbed by the more distant planets, but *may* be perturbed by either the planets or the moons, once planetary orbit crossing commences, exciting the planets and liberating the moons. To test this scenario, we inject an annular distribution of test particles with $a_{\rm belt} = 1.0$ au into the example simulation illustrated in Fig. 1. We then integrate the simulation to understand whether the scattered moons disrupt the annulus. We integrate the simulations from $t = 10^7$ yr (just prior to the onset of scattering in Fig. 1) for a further 10^7yr, and plot the subsequent evolution of the particles in Fig. 5.

In Fig. 5, the belt is initially located at $a_{\rm belt} = 1.0$ au (red circles). The final state of the belt is plotted using black squares. In the top panel, we show a Cartesian snapshot of the belt, illustrating the initial conditions and the final positions at $t = 10^7$ yr. In the bottom panel, we show the a and q values. The belt is excited to pericentres ∼0.01 au within 10 Myr by perturbations from the scattered moons.

We also repeated the experiment for a belt with $a_{\rm belt} = 0.3$ au (*not* illustrated), and found that such a belt was *not* significantly excited by the scattered moons.

We find that, for certain configurations of small-body populations, it is possible for liberated moons to excite the bodies on to orbits which cross the white dwarf's Roche radius.

6 DISCUSSION

Our results show that liberated moons more easily create a constantly changing dynamic environment than do planets alone. Exomoons are regularly perturbed within 10^{-1} au or even 10^{-2} au of the white dwarf. As discussed in Section 4, many moons remain bound at 10^8 yr (Fig. 2), and planet–planet collisions continue on Gyr time-scales; hence, any moons which may happen to remain bound to their parent planet after 100 Myr (the period of time we simulate) may still be ejected at later times. Moreover, the chaotic nature of the scattering of small bodies (liberated moons on heliocentric orbits) by planets on crossing orbits naturally means that over time a greater range of parameter space will be explored, leading to a greater chance of small pericentre orbits being explored by liberated moons.

When moons are scattered to very small pericentres (Section 4), they may become tidally disrupted (Section 5.1). This is of particular relevance, given the non-trivial fraction of simulation time in which we observe moons close to the WD (see Fig. 3), suggesting that such interactions could have a significant integrated effect.

Consequently, the moons might represent pollutants themselves. For example, one (speculative) origin for the observed debris in the WD 1145+017 system (Vanderburg et al. 2015) is that a moon is a direct cause of one or more transits. If so, then it would likely have been circularized, perhaps through some combination of tides and/or gas drag.

Such a scenario escapes one of the significant challenges of explaining observed accretion rates with asteroids, which is that, on average, exoasteroid belts would need to be about 10^3 as massive as the Solar system asteroid belt (Debes et al. 2012). Moons provide a larger reservoir, as the total mass in moons in the Solar system is about two orders of magnitude larger than the mass in the asteroid belt.

Alternatively, a moon could act as a perturbing mechanism for smaller bodies to be scattered close to white dwarfs such as WD 1145+017. One mechanism by which this may occur is for a more distant population such as the Kuiper belt. While it has been demonstrated that such a population can explain accretion rates (Bonsor et al. 2011), perturbed Kuiper belt objects have not yet been shown to reach the small target of the white dwarf itself. In this respect, liberated moons meandering within 1 au may provide a crucial component of the conveyor belt provided by the remaining planets (Bonsor & Wyatt 2012). Such moons may also increase the efficiency rate of cometary impacts (Alcock, Fristrom & Siegelman 1986; Veras & Wyatt 2012; Veras, Shannon & Gänsicke 2014d; Veras et al. 2014a; Stone, Metzger & Loeb 2015), although compositionally comets remain disfavoured (Klein et al. 2010, 2011; Gänsicke et al. 2012; Jura et al. 2012; Xu et al. 2013, 2014; Wilson et al. 2015) even for progenitors which are thought to be water rich (Farihi, Gänsicke & Koester 2013; Raddi et al. 2015).

An alternative mechanism could be for a small-body population at relatively small semimajor axis (e.g. 0.01–1.0 au) to be directly perturbed by the moon during its small pericentre incursions. In Section 5.2, we demonstrated that such scattering of interior asteroid/debris belts can indeed occur. However, the existence of such a population after the significant stellar expansion of the giant branch is highly speculative.

The moons themselves are highly unlikely to significantly affect the orbits of one another because of their small masses, unless they have already reached the white dwarf disruption radius (and have started to break up). For example, for multiple Ceres-mass and lower co-orbital bodies with orbital periods of just about 4.5 h, the resulting orbital period deviations due to their mutual perturbations are of the order of seconds (Gurri et al. 2017; Veras, Marsh & Gänsicke 2016b). This deviation is observationally relevant for the WD 1145+017 system (Gänsicke et al. 2016; Gary et al. 2016; Rappaport et al. 2016), but only because these orbits are so compact. Mutual perturbations amongst moons are primarily important during the formation of the moons themselves and their subsequent evolution around their parent planet; in our Solar system, there exist several relevant examples (e.g. Io, Europa and Ganymede, and Mimas and Tethys). Also irrelevant are long-range interactions between planets, as they have been demonstrated (Payne et al. 2013) to have little effect on the stability of moons: it is the hard scattering between planets that causes the liberation of moons (Payne et al. 2016).

7 CONCLUSIONS

With the knowledge that liberating moons from their parent planet during the white dwarf phase is a common process (Payne et al. 2016), here we have tracked the fate of these moons. We find the following.

(i) Liberated moons can easily become minor planets.

(ii) Liberated moons more easily meander about the inner reaches (within 1 au) of a white dwarf system than their parent planets.

(iii) The minimum pericentre achieved by the liberated moons, even after just 10^8 yr, is typically under 10^{-2} au.

Consequently, the liberated moons may act as *either* a direct source of pollutant material, or the innermost component of a conveyor belt which allows smaller bodies in the system (such as asteroids) to be perturbed on to the white dwarf (Bonsor & Wyatt 2012). As seen in Fig. 2, many moons remain bound after the 10^8 yr modelled here, yet planet–planet scattering around WDs continues over Gyr time-scales (Veras & Gänsicke 2015), providing further opportunity for liberation of moons. Hence, the prevalence of moons in inner regions is likely to increase as these systems are tracked over longer timespans.

We do not intend this paper to represent an accurate gauge of the fraction of moons that become unbound, but rather as a qualitative assessment of what can happen to moons once they become unbound in white dwarf systems, demonstrating that they can and do go on to repeatedly experience very close-pericentre encounters with the white dwarf. Further work will be required to understand the relative importance of liberated moon material compared to other potential sources (asteroidal, cometary, and planetary) in polluted white dwarf systems.

ACKNOWLEDGEMENTS

The authors thank the anonymous referees for their comments and suggestions. All authors gratefully acknowledge the Royal Society, whose funding (grant number IE140641) supported the research leading to these results. MJP also acknowledges NASA Origins of Solar Systems Program grant NNX13A124G, NASA Origins of Solar Systems Program grant NNX10AH40G via subaward agreement 1312645088477, NASA Solar System Observations grant NNX16AD69G, BSF grant number 2012384, as well as support from the Smithsonian 2015 CGPS/Pell Grant program. DV and BTG were also benefited by support from the European Union through ERC grant number 320964.

REFERENCES

Adams F. C., Bloch A. M., 2013, ApJ, 777, L30
Alcock C., Fristrom C. C., Siegelman R., 1986, ApJ, 302, 462
Alonso R., Rappaport S., Deeg H. J., Palle E., 2016, A&A, 589, 7
Antoniadou K. I., Veras D., 2016, MNRAS, 463, 4108
Bear E., Soker N., 2013, New Astron., 19, 56
Bonsor A., Wyatt M. C., 2012, MNRAS, 420, 2990
Bonsor A., Mustill A. J., Wyatt M. C., 2011, MNRAS, 414, 930
Chambers J. E., 1999, MNRAS, 304, 793
Croll B. et al., 2016, ApJ, preprint (arXiv:1510.06434)
Debes J. H., Hoard D. W., Wachter S., Leisawitz D. T., Cohen M., 2011, ApJS, 197, 38
Debes J. H., Walsh K. J., Stark C., 2012, ApJ, 747, 148
Dufour P. et al., 2007, ApJ, 663, 1291
Dufour P., Kilic M., Fontaine G., Bergeron P., Melis C., Bochanski J., 2012, ApJ, 749, 6
Efroimsky M., Makarov V. V., 2013, ApJ, 764, 26
Faedi F., West R. G., Burleigh M. R., Goad M. R., Hebb L., 2011, MNRAS, 410, 899
Farihi J., 2016, New Astron. Rev., 71, 9
Farihi J., Gänsicke B. T., Steele P. R., Girven J., Burleigh M. R., Breedt E., Koester D., 2012, MNRAS, 421, 1635
Farihi J., Gänsicke B. T., Koester D., 2013, Science, 342, 218
Frewen S. F. N., Hansen B. M. S., 2014, MNRAS, 439, 2442
Fulton B. J. et al., 2014, ApJ, 796, 114
Gänsicke B. T., 2011, AIP Conf. Ser., Vol. 1331, Planetary Systems Beyond the Main Sequence. Am. Inst. Phys., New York, p. 211
Gänsicke B. T., Marsh T. R., Southworth J., Rebassa-Mansergas A., 2006, Science, 314, 1908
Gänsicke B. T., Marsh T. R., Southworth J., 2007, MNRAS, 380, L35
Gänsicke B. T., Koester D., Marsh T. R., Rebassa-Mansergas A., Southworth J., 2008, MNRAS, 391, L103
Gänsicke B. T., Koester D., Farihi J., Girven J., Parsons S. G., Breedt E., 2012, MNRAS, 424, 333
Gänsicke B. T. et al., 2016, ApJ, 818, 6
Gary B. L., Rappaport S., Kaye T. G., Alonso R., Hambsch F.-J., 2016, MNRAS, preprint (arXiv:1608.00026)
Gentile Fusillo N. P., Gänsicke B. T., Greiss S., 2015, MNRAS, 448, 2260
Graham J. R., Matthews K., Neugebauer G., Soifer B. T., 1990, ApJ, 357, 216
Guo J., Tziamtzis A., Wang Z., Liu J., Zhao J., Wang S., 2015, ApJ, 810, L17
Gurri P., Veras D., Gänsicke B. T., 2017, MNRAS, 464, 321
Henning W. G., Hurford T., 2014, ApJ, 789, 30
Hogan E., Burleigh M. R., Clarke F. J., 2009, MNRAS, 396, 2074
Jura M., 2003, ApJ, 584, L91
Jura M., Young E. D., 2014, Annu. Rev. Earth Planet. Sci., 42, 45
Jura M., Xu S., Klein B., Koester D., Zuckerman B., 2012, ApJ, 750, 69
Kepler S. O. et al., 2015, MNRAS, 446, 4078
Kepler S. O. et al., 2016, MNRAS, 455, 3413
Klein B., Jura M., Koester D., Zuckerman B., Melis C., 2010, ApJ, 709, 950
Klein B., Jura M., Koester D., Zuckerman B., 2011, ApJ, 741, 64
Kleinman S. J. et al., 2013, ApJS, 204, 5
Koester D., Gänsicke B. T., Farihi J., 2014, A&A, 566, A34
Kunitomo M., Ikoma M., Sato B., Katsuta Y., Ida S., 2011, ApJ, 737, 66
Li G., Naoz S., Kocsis B., Loeb A., 2014, ApJ, 785, 116

Manser C. J. et al., 2016, MNRAS, 455, 4467
Matsumura S., Ida S., Nagasawa M., 2013, ApJ, 767, 129
Melis C. et al., 2012, ApJ, 751, L4
Metzger B. D., Rafikov R. R., Bochkarev K. V., 2012, MNRAS, 423, 505
Mullally F., Winget D. E., Degennaro S., Jeffery E., Thompson S. E., Chandler D., Kepler S. O., 2008, ApJ, 676, 573
Mustill A. J., Villaver E., 2012, ApJ, 761, 121
Mustill A. J., Veras D., Villaver E., 2014, MNRAS, 437, 1404
Nordhaus J., Spiegel D. S., 2013, MNRAS, 432, 500
Payne M. J., Deck K. M., Holman M. J., Perets H. B., 2013, ApJ, 775, L44
Payne M. J., Veras D., Holman M. J., Gänsicke B. T., 2016, MNRAS, 457, 217
Raddi R., Gänsicke B. T., Koester D., Farihi J., Hermes J. J., Scaringi S., Breedt E., Girven J., 2015, MNRAS, 450, 2083
Rafikov R. R., 2011a, MNRAS, 416, L55
Rafikov R. R., 2011b, ApJ, 732, L3
Rafikov R. R., Garmilla J. A., 2012, ApJ, 760, 123
Rappaport S., Gary B. L., Kaye T., Vanderburg A., Croll B., Benni P., Foote J., 2016, MNRAS, 458, 3904
Raymond S. N., Armitage P. J., Gorelick N., 2010, ApJ, 711, 772
Redfield S., Farihi J., Cauley P. W., Parsons S. G., Gaensicke B. T., Duvvuri G., 2016, ApJ, preprint (arXiv:1608.00549)
Sandhaus P. H., Debes J. H., Ely J., Hines D. C., Bourque M., 2016, ApJ, 823, 15
Schatzman E., 1945, Ann. d'Astrophys., 8, 143
Staff J. E., De Marco O., Wood P., Galaviz P., Passy J.-C., 2016, MNRAS, 458, 832
Steele P. R., Burleigh M. R., Dobbie P. D., Jameson R. F., Barstow M. A., Satterthwaite R. P., 2011, MNRAS, 416, 2768
Stone N., Metzger B. D., Loeb A., 2015, MNRAS, 448, 188
Vanderburg A. et al., 2015, Nature, 526, 546
Veras D., 2016a, R. Soc. Open Sci., 3, 150571
Veras D., 2016b, MNRAS, 463, 2958
Veras D., Armitage P. J., 2005, ApJ, 620, L111
Veras D., Gänsicke B. T., 2015, MNRAS, 447, 1049
Veras D., Wyatt M. C., 2012, MNRAS, 421, 2969
Veras D., Mustill A. J., Bonsor A., Wyatt M. C., 2013, MNRAS, 431, 1686
Veras D., Evans N. W., Wyatt M. C., Tout C. A., 2014a, MNRAS, 437, 1127
Veras D., Leinhardt Z. M., Bonsor A., Gänsicke B. T., 2014b, MNRAS, 445, 2244
Veras D., Jacobson S. A., Gänsicke B. T., 2014c, MNRAS, 445, 2794
Veras D., Shannon A., Gänsicke B. T., 2014d, MNRAS, 445, 4175
Veras D., Eggl S., Gänsicke B. T., 2015a, MNRAS, 451, 2814.
Veras D., Leinhardt Z. M., Eggl S., Gänsicke B. T., 2015b, MNRAS, 451, 3453.
Veras D., Eggl S., Gänsicke B. T., 2015c, MNRAS, 452, 1945
Veras D., Mustill A. J., Gänsicke B. T., Redfield S., Georgakarakos N., Bowler A. B., Lloyd M. J. S., 2016a, MNRAS, 458, 3942
Veras D., Marsh T. R., Gänsicke B. T., 2016b, MNRAS, 461, 1413
Veras D., Carter P. J., Leinhardt Z. L., Gänsicke B. T., 2016c, MNRAS, submitted
Villaver E., Livio M., 2009, ApJ, 705, L8
Villaver E., Livio M., Mustill A. J., Siess L., 2014, ApJ, 794, 3
Wilson D. J., Gänsicke B. T., Koester D., Toloza O., Pala A. F., Breedt E., Parsons S. G., 2015, MNRAS, 451, 3237
Xu S., Jura M., Klein B., Koester D., Zuckerman B., 2013, ApJ, 766, 132
Xu S., Jura M., Koester D., Klein B., Zuckerman B., 2014, ApJ, 783, 79
Xu S., Jura M., Dufour P., Zuckerman B., 2016, ApJ, 816, 6
Zuckerman B., Koester D., Reid I. N., Hünsch M., 2003, ApJ, 596, 477
Zuckerman B., Melis C., Klein B., Koester D., Jura M., 2010, ApJ, 722, 725

This paper has been typeset from a TEX/LATEX file prepared by the author.